Synthesis, X-ray Structure, and Electrochemical and Excited-State Properties of Multicomponent Complexes Made of a $[Ru(Tpy)_2]^{2+}$ Unit Covalently Linked to a [2]-Catenate Moiety. Controlling the Energy-Transfer Direction by Changing the Catenate Metal Ion

Diego J. Cárdenas,[†] Jean-Paul Collin,[†] Pablo Gaviña,[†] Jean-Pierre Sauvage,*[,†] André De Cian,[‡] Jean Fischer,[‡] Nicola Armaroli,*[,§] Lucia Flamigni,[§] Veronica Vicinelli,[⊥] and Vincenzo Balzani*[,⊥]

Contribution from the Laboratoire de Chimie Organo-Minérale, UMR7513 ULP/CNRS, Institut de Chimie, Université Louis Pasteur, 4 rue Blaise Pascal, F-67070 Strasbourg, France, Laboratoire de Cristallochimie et de Chimie Structurale, UMR7513 ULP/CNRS, Institut de Chimie, Université Louis Pasteur, 4 rue Blaise Pascal, F-67070 Strasbourg, France, Istituto FRAE-CNR, via Gobetti 101, 40129 Bologna, Italy, and Dipartimento di Chimica "G. Ciamician", Università di Bologna, via Selmi 2, 40126 Bologna, Italy

Received January 4, 1999

Abstract: New multicomponent species consisting of [2]-catenates incorporating the $[Ru(tpy)_2]^{2+}$ moiety (tpy = 2,2′:6′,2″-terpyridine) within their framework have been prepared, and their electrochemical and photophysical properties have been studied. The parent compound of the investigated species is a previously described Cu(I) catenate (**RuCu**) containing a $[Cu(dap)_2]^+$ fragment (dap = 2,9-dianisyl-1,10-phenanthroline) used as a template and a $[Ru(tpy)_2]^{2+}$ unit integrating one of the interlocked rings. Selective demetalation of the Cu(I) catenate moiety of **RuCu** afforded a catenand (**Ru**) containing the $[Ru(tpy)_2]^{2+}$-type component and a free tetrahedral coordination site. Reaction of this catenand with Ag^+ and Zn^{2+} ions yielded two new bimetallic catenates (**RuAg** and **RuZn**, respectively). The solid-state structure of complexes **RuCu** and **RuAg** has been determined by X-ray diffraction. Electrochemical experiments have shown that the two moieties of the **RuCu** and **RuAg** catenates undergo independent redox processes. The photophysical properties of **Ru**, **RuCu**, **RuZn**, and **RuAg** have been investigated by steady-state and time-resolved techniques, and compared with those of appropriate model compounds. The absorption spectra do not show any appreciable ground-state electronic interactions between the [2]-catM (cat = catenand, catM = catenate) and $[Ru(tpy)_2]^{2+}$-type moieties, whereas luminescence properties reveal the occurrence of efficient photoinduced intercomponent energy- and/or electron-transfer processes, whose direction depends on the presence or on the nature of the metal ion in the [2]-cat-type moiety. In **Ru, RuZn**, and **RuAg** such a moiety is quenched by the $[Ru(tpy)_2]^{2+}$ unit, whereas for **RuCu** the opposite behavior is observed. The rate constant of intercomponent processes are determined via time-resolved nano- and picosecond luminescence spectroscopy.

Introduction

Much attention is currently devoted to the synthesis and properties of rotaxanes, catenanes, and related species.[1−6] One of the most important properties of these compounds, which contain threaded or interlocked components, is their ability to undergo mechanical motions under the action of chemical,[7] electrochemical,[8] or photochemical[9] stimulation (molecular-level mechanical machines).[10] Incorporation in such supramolecular species of Ru(II)−polypyridine units, which exhibit outstanding electrochemical and excited-state properties,[11,12] may open the way to new kinds of electrochemically- and light-driven molecular machines as well as to supramolecular species capable of conducting electrons or electronic energy over long dis-

[†] Laboratoire de Chimie Organo-Minérale, Université Louis Pasteur.
[‡] Laboratoire de Cristallochimie et de Chimie Structurale, Université Louis Pasteur.
[§] Istituto FRAE-CNR.
[⊥] Università di Bologna.

(1) Chambron, J.-C.; Dietrich Buchecker, C. O.; Sauvage, J.-P. In *Comprehensive Supramolecular Chemistry*; Lehn J.-M., Ed.; Pergamon Press: Oxford, 1996; Vol. 9, p 43.
(2) Amabilino, D. B.; Stoddart, J. F. *Chem. Rev.* **1995**, *95*, 2725.
(3) Vögtle, F.; Jäger, R.; Händel, M.; Ottens-Hildebrandt, S. *Pure Appl. Chem.* **1996**, *68*, 225. (b) Vögtle, F.; Dünnwald, T.; Schmidt, T. *Acc. Chem. Res.* **1996**, *29*, 451.
(4) Hamilton, D. G.; Davies, J. E.; Prodi, L.; Sanders, J. K. M. *Chem. Eur. J.* **1998**, *4*, 608.
(5) Li, Z.-T.; Stein, P. C.; Becher, J.; Jensen, D.; Mork, P.; Svenstrup, N. *Chem. Eur. J.* **1996**, *2*, 624.
(6) Leigh, D. A.; Murphy, A.; Smart, J. P.; Slawin, A. M. Z. *Angew. Chem., Int. Ed. Engl.* **1997**, *36*, 728.
(7) For leading references see: (a) Bissell, R. A.; Córdova, E.; Kaifer, A. E.; Stoddart, J. F. *Nature* **1994**, *369*, 133. (b) Amabilino, D. B.; Dietrich-Buchecker, C. O.; Livoreil, A.; Pérez-Garcìa, L.; Sauvage, J.-P.; Stoddart, J. F. *J. Am. Chem. Soc.* **1996**, *118*, 3905. (c) Ballardini, R.; Balzani, V.; Credi, A.; Gandolfi, M. T.; Langford, S. J.; Menzer, S.; Prodi, L.; Stoddart, J. F.; Venturi, M.; Williams, D. J. *Angew. Chem., Int. Ed. Engl.* **1996**, *35*, 978. (d) Credi, A.; Balzani, V.; Langford, S. J.; Stoddart, J. F. *J. Am. Chem. Soc.* **1997**, *119*, 2679. (e) Ashton, P. R.; Ballardini, R.; Balzani, V.; Gomez-Lopez, M.; Lawrence, S. E.; Martinez-Diaz, M. V.; Montalti, M.; Piersanti, A.; Prodi, L.; Stoddart, J. F.; Williams, D. J. *J. Am. Chem. Soc.* **1997**, *119*, 10641. (f) Credi, A.; Montalti, M.; Balzani, V.; Langford, S. J.; Raymo, F. M.; Stoddart, J. F. *New J. Chem.* **1998**, 1061. (g) Ashton, P. R.; Ballardini, R.; Balzani, V.; Fyfe, M. C. T.; Gandolfi, M. T.; Martinez-Diaz, M. V.; Morosini, M.; Schiavo, C.; Shibata, K.; Stoddart, J. F.; White A. J. P.; Williams, D. J. *Chem. Eur. J.* **1998**, *4*, 2332.

10.1021/ja990036v CCC: $18.00
Published on Web 05/27/1999

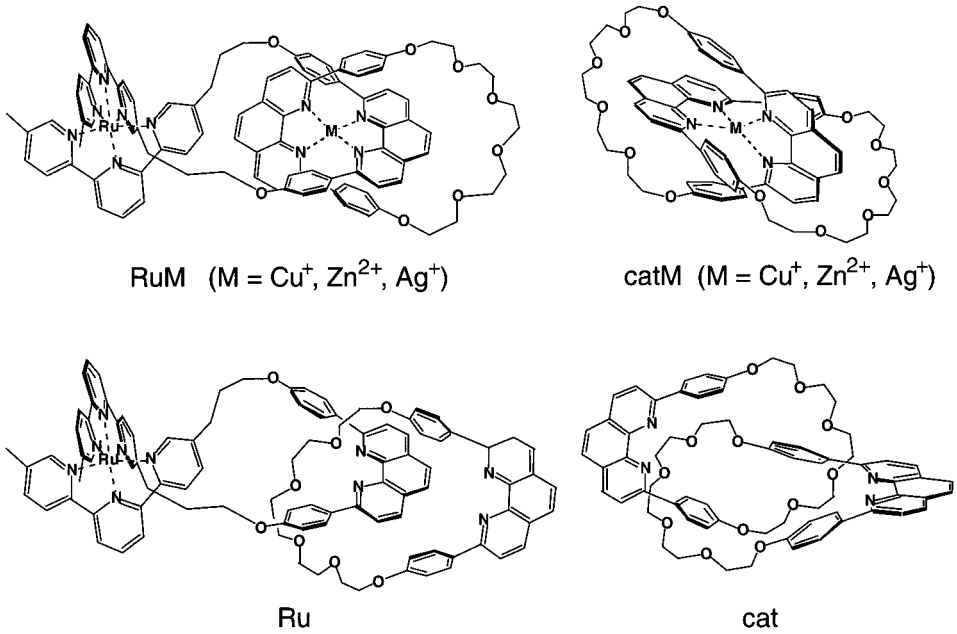

Figure 1. Structural formulas of the investigated compounds (left-hand side) and of the models of their catenane-type moieties.

tances.[13] In an attempt to explore some synthetic routes along these directions, we have synthesized the compounds **Ru**,[14] **RuCu**,[14] **RuAg**, and **RuZn** shown in Figure 1. Such compounds are examples of [2]-catenane structures where one of the two rings is closed by coordination bonds; the ensuing coordination geometry is quite unusual, as a tetrahedral and an octahedral metal center are located on the same compound. From a supramolecular viewpoint, the investigated RuM systems (Figure 1) are clearly made of two moieties, namely, a $[Ru(tpy)_2]^{2+}$-type (tpy = 2,2′:6′,2″-terpyridine) complex and a [2]-catenate ($M = Cu^+$, Ag^+, and Zn^{2+}) or a [2]-catenand (M = nothing). For **RuCu** and **RuAg**, single crystals suitable for X-ray diffraction could be obtained, and their solid-state structures have been determined. The electrochemical and excited-state properties of **Ru**, **RuCu**, **RuZn**, and **RuAg** have been investigated and compared with the properties exhibited by the model compounds of their subunits. Such models are the previously investigated $[Ru(tpy)_2]^{2+}$ complex,[12,15] a [2]-catenand (cat),[16] and [2]-catenates (catCu, catAg, and catZn),[16] also shown in Figure 1. One aim of this work was to take advantage of the tunability of the energy levels of the catM moiety on changing the nature of the metal ion, to switch the direction of the energy transfer between the two components of the supramolecular structure.

Experimental Section

General Methods. Thin-layer chromatography (TLC) was carried out on aluminum sheets coated with silica gel 60 (Merck 5554). ^{1}H NMR spectra were recorded on either a Brucker WP 200SY (200 MHz) or a Brucker WP 400SY (400 MHz) spectrometer (using the deuterated solvent as the lock and the residual solvent as the internal reference). Fast atom bombardment mass spectra (FAB-MS) were recorded in the positive ion mode with either a krypton primary atom beam in conjunction with a 3-nitrobenzyl alcohol matrix and a Kratos MS80RF mass spectrometer coupled to a DS90 system or a xenon primary atom beam with the same matrix and a ZAB-HF mass spectrometer.

Synthesis of Catenand Ru and Copper(I) Catenate RuCu. The formulas are $[RuC_{96}H_{84}N_{10}O_8(PF_6)_2]$ and $[RuCuC_{96}H_{84}N_{10}O_8(PF_6)_3]$, respectively; the synthesis of these compounds has been previously reported.[14]

Synthesis of Zinc(II) Catenate RuZn ($[RuZnC_{96}H_{84}N_{10}O_8(PF_6)_4]$). $Zn(NO_3)_2 \cdot 3H_2O$ (3.8 mg, 0.016 mmol) in MeOH (2 mL) was added with stirring to a solution of free catenand **Ru** (28 mg, 0.0148 mmol) in CH_2Cl_2 (5 mL) at room temperature. TLC (SiO_2; $MeCN-H_2O$, 9:1, and 0.5% saturated aqueous KNO_3) showed the immediate disappear-

(8) For leading references see: (a) Livoreil, A.; Dietrich-Buchecker, C. O.; Sauvage, J.-P. *J. Am. Chem. Soc.* **1994**, *116*, 9399. (b) Ashton, P. R.; Ballardini, R.; Balzani, V.; Credi, A.; Gandolfi, M. T.; Menzer, S.; Pérez-García, L.; Prodi, L.; Stoddart, J. F.; Venturi, M.; White, A. J. P.; Williams, D. J. *J. Am. Chem. Soc.* **1995**, *117*, 11171. (c) Collin, J.-P.; Gaviña, P.; Sauvage, J.-P. *J. Chem. Soc., Chem. Commun.* **1996**, 2005. (d) Ashton, P. R.; Ballardini, R.; Balzani, V.; Boyd, S. E.; Credi, A.; Gandolfi, M. T.; Gómez-López, M.; Iqbal, S.; Philp, D.; Preece, J. A.; Prodi, L.; Ricketts, H. G.; Stoddart, J. F.; Tolley, M. S.; Venturi, M.; White, A. J. P.; Williams, D. J. *Chem. Eur. J.* **1997**, *3*, 152. (e) Cárdenas, D. J.; Livoreil, A.; Sauvage, J.-P. *J. Am. Chem. Soc.* **1996**, *118*, 11980. (f) Asakawa, M.; Ashton, P.; Balzani, V.; Credi, A.; Mattersteig, G.; Matthews, O. A.; Montalti, M.; Spencer, N.; Stoddart, J. F.; Venturi, M. *Chem. Eur. J.* **1997**, *3*, 1992. (g) Livoreil, A.; Sauvage, J.-P.; Armaroli, N.; Balzani, V.; Flamigni, L.; Ventura, B. *J. Am. Chem. Soc.* **1997**, *119*, 12114. (h) Asakawa, M.; Ashton, P.; Balzani, V.; Credi, A.; Hamers, C.; Mattersteig, G.; Montalti, M.; Shipway, A. N.; Spencer, N.; Stoddart, J. F.; Tolley, M. S.; Venturi, M.; White, A. J. P.; Williams, D. J. *Angew. Chem., Int. Ed. Eng.* **1998**, *37*, 333.

(9) For leading references see: (a) Ballardini, R.; Balzani, V.; Gandolfi, M. T.; Prodi, L.; Venturi, M.; Philp, D.; Ricketts, H. G.; Stoddart, J. F. *Angew. Chem., Int. Ed. Engl.* **1993**, *32*, 1301. (b) Bauer, M.; Müller, W. M.; Müller, U.; Rissanen, K.; Vögtle, F. *Liebigs Ann.* **1995**, 649. (c) Benniston, A. C.; Harriman, A.; Lynch, V. M. *J. Am. Chem. Soc.* **1995**, *117*, 5275.

(10) For recent reviews see: (a) Benniston, A. C. *Chem. Soc. Rev.* **1996**, *25*, 427. (b) Balzani, V.; Gomez-Lopez, M.; Stoddart, J. F. *Acc. Chem. Res.* **1998**, *31*, 405. (c) Sauvage, J.-P. *Acc. Chem. Res.* **1998**, *31*, 611.

(11) (a) Juris, A.; Balzani, V.; Barigelletti, F.; Campagna, S.; Belser, P.; von Zelewsky, A. *Coord. Chem. Rev.* **1988**, *84*, 85. (b) Balzani, V.; Juris, A.; Venturi, M.; Campagna, S.; Serroni, S. *Chem. Rev.* **1996**, *96*, 759.

(12) Sauvage, J.-P.; Collin, J.-P.; Chambron, J.-C.; Guillerez, S.; Coudret, C.; Balzani, V.; Barigelletti, F.; De Cola, L.; Flamigni, L *Chem. Rev.* **1994**, *94*, 993.

(13) (a) Balzani, V.; Barigelletti, F.; Belser, P.; Bernhard, S.; De Cola, L.; Flamigni, L. *J. Phys. Chem.* **1996**, *100*, 16786. (b) Barigelletti, F.; Flamigni, L.; Balzani, V.; Collin, J.-P.; Sauvage, J.-P.; Sour, A.; Constable, E. C.; Cargill-Thompson, A. M. W. *J. Am. Chem. Soc.* **1994**, *116*, 7692. (c) Barigelletti, F.; Flamigni, L.; Balzani, V.; J.-P. Collin; Sauvage, J.-P.; Sour, A. *New J. Chem.* **1995**, *19*, 793. (d) Collin, J.-P.; Gaviña, P.; Heitz, V.; Sauvage, J.-P. *Eur. J. Inorg. Chem.* **1998**, *1*, 1. (e) Armaroli, N.; Diederich, F.; Dietrich-Buchecker, C. O.; Flamigni, L.; Marconi, G.; Nierengarten, J.-F.; Sauvage, J.-P. *Chem. Eur. J.* **1998**, *4*, 406.

(14) Cárdenas, D. J.; Gaviña, P.; Sauvage, J.-P. *J. Am. Chem. Soc.* **1997**, *119*, 2656.

(15) Maestri, M.; Armaroli, N.; Balzani, V.; Constable, E. C.; Cargill-Thompson, A. M. W. *Inorg. Chem.* **1995**, *34*, 2759.

(16) Armaroli, N.; De Cola, L.; Balzani, V.; Sauvage, J.-P.; Dietrich-Buchecker, C. O.; Kern, J.-M.; Bailal, A. *J. Chem. Soc., Dalton Trans.* **1993**, 3241.

ance of the starting complex. The mixture was left with stirring overnight. The solvent was evaporated, and the residue was dissolved in MeCN. Then KPF_6 was added, followed by an excess of H_2O to precipitate the complex as its PF_6^- salt. The product was further purified by column chromatography on silica gel (MeCN−H_2O, 9:1, containing 0−1% saturated aqueous KNO_3) and isolated as its PF_6^- salt (23 mg, 74%): ^{1}H NMR (acetone-d_6, 400 MHz) δ 9.12 (d, J = 8.3 Hz, 2H), 9.09 (d, J = 8.0 Hz, 2H), 9.06 (d, J = 8.3 Hz, 2H), 9.01 (d, J = 8.0 Hz, 2H), 8.70 (d, J = 8.3 Hz, 2H), 8.68 (s, 2H), 8.58 (t, J = 8.0 Hz, 2H), 8.30 (d, J = 8.3 Hz, 2H), 8.22 (d, J = 8.6 Hz, 2H), 8.15 (dd, J = 8.3 and 1.9 Hz, 2H), 8.13 (d, J = 8.3 Hz, 2H), 7.92 (d, J = 1.3 Hz, 2H), 7.91 (dd, J = 8.3 and 1.1 Hz, 2H), 7.58 (d, J = 1.9 Hz, 2H), 7.49 (d, J = 8.7 Hz, 4H), 7.48 (d, J = 8.7 Hz, 4H), 6.33 (s, 2H), 6.32 (d, J = 8.7 Hz, 4H), 6.31 (d, J = 8.7 Hz, 4H), 3.85 (s, 4H), 3.72 (m, 8H), 3.54 (m, 8H), 3.41 (m, 4H), 2.34 (t, J = 7.5 Hz, 4H), 2.07 (s, 6H), 1.29 (m, 4H); FAB-MS m/z 2107.1 ([M − PF_6]$^+$, calcd 2107.1), 1961.1 ([M − $2PF_6$]$^+$, calcd 1962.1), 1816.2 ([M − $3PF_6$]$^+$, calcd 1817.2).

Silver(I) Catenate RuAg [$RuAgC_{96}H_{84}N_{10}O_8(PF_6)_3$]. A solution of $AgBF_4$ (4.7 mg, 0.024 mmol) in acetone (2 mL) was added to a deoxygenated solution of **Ru** (30.3 mg, 0.016 mmol) in acetone (2 mL) at room temperature, and the mixture was stirred under Ar for 2 h in the dark. The acetone was evaporated, and the residue was taken in CH_2Cl_2 and washed with H_2O. Then CH_2Cl_2 was removed, and the residue was dissolved in MeCN and treated with an excess of saturated aqueous KPF_6 with stirring. The MeCN was evaporated and the residue taken again into CH_2Cl_2 and washed with more H_2O. Evaporation of the solvent led to a red solid which was dried under vacuum overnight to yield the desired silver(I) catenate (35 mg, quantitative): ^{1}H NMR (acetone-d_6, 200 MHz) δ 9.09 (d, J = 8.0 Hz, 2H), 9.03 (d, J = 8.3 Hz, 2H), 8.95 (d, J = 8.2 Hz, 2H), 8.79 (d, J = 8.3 Hz, 2H), 8.70 (d, J = 8.2 Hz, 2H), 8.62 (t, J = 8.1 Hz, 2H), 8.40 (s, 2H), 8.06 (d, J = 8.3 Hz, 2H), 7.98 (br s, 2H), 7.90 (br d, $J \sim$ 8.4 Hz, 2H), 7.69 (br d, $J \sim$ 8.3 Hz, 2H), 7.57 (d, J = 8.3 Hz, 2H), 7.53 (br s, 2H), 7.50 (s, 2H), 7.40 (d, J = 8.7 Hz, 4H), 7.31 (d, J = 8.3 Hz, 2H), 7.25 (d, J = 8.7 Hz, 4H), 6.20 (d, J = 8.7 Hz, 4H), 6.12 (d, J = 8.7 Hz, 4H), 3.79 (s, 4H), 3.60−3.15 (m, 20H), 2.32−2.19 (m, 4H), 2.07 (s, 6H), 1.10−1.12 (m, 4H); FAB-MS m/z 2005.2 ([M − PF_6]$^+$, calcd 2005.4), 1858.2 ([M − $2PF_6$]$^+$, calcd 1858.4), 1712.2 ([M − $3PF_6$]$^+$).

Electrochemical Measurements. Electrochemical experiments were performed with a three-electrode system consisting of a platinum working electrode or a hanging mercury working electrode (HME), a platinum-wire counter electrode, and a standard reference saturated calomel electrode (SCE), versus which all potentials are reported. All measurements were carried out under Ar, in degassed spectroscopic grade MeCN (previously distilled from CaH_2 under Ar) or CH_2Cl_2 (distilled from CaH_2 or P_2O_5 under Ar), using 0.1 M n-Bu_4NBF_4 solutions as the supporting electrolyte. An EG&G Princeton Applied Research Model 273A potentiostat connected to a computer (Programme Research Electrochemistry Software) and a Brucker EI 30M potentiostat connected to a printing table were used for the cyclic voltammetry (CV) measurements.

X-ray Crystallography. The crystal data for **RuCu**·$(MeCN)_2$·$(MeOH)_3$·H_2O were collected at −100 °C in the $\theta/2\theta$ flying step scan mode with a crystal of 0.40 × 0.40 × 0.40 mm^3 dimensions on a Philips PW1100/16 diffractometer using graphite-monochromated Cu Kα radiation (λ = 1.5418 Å). For **RuAg**·$(C_6H_6)_5$·H_2O, crystal data were collected at −100 °C in the $\theta/2\theta$ scan mode with a crystal of 0.40 × 0.40 × 0.40 mm^3 dimensions on a Nonius CAD4-F diffractometer using graphite-monochromated Mo Kα radiation (λ = 0.710 73 Å). For both compounds, X-ray experimental data are given in Table 1. The unit cell parameters have been refined using 24 and 25 high-angle reflections for **RuCu** and **RuAg**, respectively. For **RuCu**, a total of 13 282 independent reflections were collected in the range 3° < θ < 54° (limit imposed by the cooling device, −18,h,17, −25,k,25, 0,l,13), from which 8946 had $I > 3\sigma(I)$. For **RuAg**, a total of 21 820 independent reflections were collected in the range 2.5° < θ < 24.6° (−20,h,20, −22,k,20, 0,l,25), from which 11 068 had $I > 3\sigma(I)$. These latter reflections were used to determine the structures by direct methods and to refine them. After isotropic refinements, a difference map showed maxima close to the positions expected for hydrogen atoms. These atoms, with the exception for **RuCu** of the solvate protons and for **RuAg** of one of the benzene rings and water protons, were included at their idealized positions as fixed contributors in structure factor calculations with a C−H = 0.95 Å and isotropic temperature factors such as B(H) = 1.3B_{equiv}(C) Å^2. At this stage, absorption corrections, using DIFABS for **RuCu** and transmission factors derived from ψ scans of seven reflections for **RuAg**, were applied (min/max transmission coefficients 0.61/1.00 for **RuCu** and 0.94/1.00 for **RuAg**). In each complex, one of the PF_6^- anions was poorly resolved. For **RuCu**, the fluorine atoms of this anion were allowed to vary as a group identical to a well-resolved PF_6^- anion. For **RuAg**, a trans pair of fluorine atoms was well resolved, but the four equatorial atoms were assigned two positions, in the ratio 1/1, rotated by 45° around the normal to the equatorial plane through P. For **RuCu**, all atoms were refined with anisotropic temperature factors, except the seven atoms of the poorly resolved PF_6^- anion and one carbon atom of the ether chain. For **RuAg**, the fluorine atoms of the disordered PF_6^- anion, the carbon atoms of two benzene rings, and the oxygen atoms of the water molecules were refined with isotropic temperature factors. Full-matrix refinements against $|F|$, with weights given by $w = 4F_o^2/[\sigma^2(F_o) + 0.0064F_o^4]$ and $w = 4F_o^2/[\sigma^2(F_o) + 0.0025F_o^4 + 5]$ for **RuCu** and **RuAg**, respectively. Final results: $R_{obsd}(F)$ = 0.083/0.068, $R_{w,obsd}(F)$ = 0.120/0.096, and GOF = 1.533/1.800. No extinction corrections were applied. A nonresolved electron-density residue of 1.4 e/Å^3 remains near the disordered PF_6^- anion of **RuCu**. All calculations were performed using the OpenMolEN package on a DEC Alpha work station.[17] Scattering factors and anomalous dispersion coefficients were taken from Cromer and Waber.[18]

Table 1. X-ray Crystallographic Experimental Data of **RuCu**$(PF_6)_3$ (**1**) and **RuAg**$(PF_6)_3$ (**2**)[a]

formula	**1**−$(CH_3CN)_2$·$(MeOH)_3$·H_2O	**2**−$(C_6H_6)_5$·H_2O
molecular weight	2301.55	2594.25
a (Å)	17.174(5)	17.742(2)
b (Å)	24.252(7)	18.85(2)
c (Å)	13.223(4)	21.564(2)
α (deg)	92.90(2)	112.265(7)
β (deg)	95.00(2)	103.620(7)
γ (deg)	91.86(2)	97.633(7)
V (Å^3)	5475(5)	6273(2)
cryst dimens (mm)	0.40 × 0.40 × 0.30	0.40 × 0.40 × 0.40
D_{calcd} (g cm^{-3})	1.40	1.37
F(000)	2364	2664
μ (mm^{-1})	2.594	0.394
trans min and max	0.53/1.00	0.94/1.00
wavelength (Å)	1.541 84	0.710 73
radiation	Cu Kα	Mo Kα
diffractometer	Philips PW1100	Nonius CAD4
hkl limits	−18,17/−25,25/0,13	−20,20/−22,20/0,25
θ limits (deg)	3.0/54.07	2.5/24.63
no. of data measd	13 282	21 820
no. of data with $I > 3\sigma(I)$	8946	11 068
no. of variables	1301	1412
R	0.084	0.068
R_w	0.121	0.097
GOF	1.533	1.800
largest peak in final diff (e Å^{-3})	1.382	0.417

[a] In common: crystal system = triclinic, space group = $P\bar{1}$, Z = 2, color = dark red, scan mode = $\theta/2\theta$, temperature = 173 K.

Photophysical Investigations. The solvents used for the absorption and luminescence studies were dichloromethane and methanol (both from Carlo Erba, spectrofluorimetric grade) or butyronitrile[19] (Fluka). Absorption spectra were recorded with a Perkin-Elmer λ5 spectrophotometer. Corrected emission spectra, and excitation spectra were

(17) OpenMoleN, Interactive Structure Solution, Nonius B.V., Delft, The Netherlands 1997.

(18) Cromer, D. T.; Waber, J. T. *International Tables for X-ray Crystallography*; The Kynoch Press: Birmingham, U.K., 1974; Vol. IV. (a) Table 2.2b. (b) Table 2.3.1.

(19) We found that phenanthroline and its derivatives undergo immediate decomposition under intense UV irradiation, when dissolved in chlorinated solvents.

obtained with a Spex Fluorolog II spectrofluorimeter equipped with continuous 150 W Xe lamp and a Hamamatsu R-928 or R-3896 (red-enhanced) photomultiplier tube. Fluorescence quantum yields were measured with the method described by Demas and Crosby[20] using $[Ru(bpy)_3]Cl_2$ in aerated water as the standard ($\Phi = 0.028$).[21] An IBH single-photon-counting apparatus (N_2 lamp, $\lambda_{exc} = 337$ nm, 1 ns time resolution) and a previously described[22] system based on a Nd:YAG laser and a Hamamatsu C1587 streak camera ($\lambda_{exc} = 532$ or 355 nm, 40 ps time resolution) were used to detect fluorescence lifetimes. Transient absorption decays were detected with a nanosecond flash photolysis apparatus, using the third harmonic of a Nd:YAG laser (355 nm) as the exciting wavelength. Details on the experimental setup are reported elsewhere.[23] When necessary, the solutions were deaerated by at least three freeze−pump−thaw cycles. Estimated experimental uncertainties are λ_{abs}, 2 nm; λ_{em}, 5 nm; τ, 10%; Φ_{em}, 20%.

Results and Discussion

Synthesis and Characterization of the Novel Compounds. In a previous paper we described[14] the preparation of catenate **RuCu** (shown in Figure 1), making use of Cu(I) as a template to thread a polyfunctional string containing a dap (2,9-dianisyl-1,10-phenanthroline) moiety and two tpy ligands in its ends into a dap-containing 30-membered macrocycle. In this way *regioselective* formation of a 4-coordinate pseudotetrahedral $[Cu(dap)_2]^+$-type complex causes the two dap subunits to adopt an intertwined structure. Ru(II) was subsequently used to effect a macrocyclization (*clipping* reaction) on the intertwined precursor by coordinating to the two free tpy moieties in a highly stable $[Ru(tpy)_2]^{2+}$-type complex. Due to the different kinetic stability of the two metal complexes, copper(I) could be selectively removed by reaction with KCN in $MeCN-H_2O$ without affecting the Ru complex, leading to catenand **Ru** which contains a free tetrahedral coordination site.[14] The new bimetallic complexes **RuZn** and **RuAg** were easily made by mixing stoichiometric amounts of the appropriate metal salt and **Ru**, followed by anion exchange with KPF_6. Both catenates were obtained as red crystalline solids. The ^1H NMR spectra of both compounds show the typical upfield shifts of the aromatic protons of the phenoxy moieties (as compared to free catenand **Ru**), due to the ring current effects of the 1,10-phenanthroline nuclei in the intertwined situation around the metal ion (**RuZn**, 6.31 and 6.32 ppm for the H meta to the phen moiety and 7.48 and 7.49 ppm for the ortho H; **RuAg**, 6.12 and 6.20 ppm for the meta H and 7.25 and 7.40 for the ortho H). This was also observed for the related catZn and catAg,[24] indicating that the system undergoes a complete rearrangement during the complexation process. FAB-MS confirmed both structures, showing peaks corresponding to the loss of PF_6- anions (calcd for [**RuZn** − $(PF_6)]^+$ 2107.1, found 2107.1; calcd for [**RuAg** − $(PF_6)]^+$ 2005.4, found 2005.2).

Electrochemistry. The results of the electrochemical measurements are summarized in Table 2. All the compounds studied show two waves corresponding to the redox processes of the Ru complex: one for the Ru(III)/Ru(II) couple at ca. +1.2 V (vs SCE) and another at ca. −1.3 V corresponding to a ligand-localized reduction. In the case of **RuCu** the potential observed for the Cu(II)/Cu(I) process (+0.58 V) is in accordance with the previously observed stabilization of Cu(I) by dap ligands.[24] For **RuAg** no signal could be detected for the reduction of Ag(I) in MeCN solution with a Pt electrode.

Table 2. Electrochemical Data[a]

	Ru(III)/Ru(II)	(tpy/tpy$^-$)[b]	M(II)/M(I)	M(I)/M(0)
Ru	1.24	−1.34		
RuCu	1.24	−1.32	0.58	
RuZn	1.27	−1.33	−0.97, ir	−1.05, ir
RuAg	1.25	−1.32		
	1.40[c]			−0.75,[c] ir

[a] $E_{1/2}$ values determined by cyclic voltammetry. Potentials (V) vs SCE. The processes are reversible except when indicated by ir (irreversible). Measurements were carried out in MeCN with a Pt electrode except as otherwise noted in footnote c. [b] Reduction of a tpy ligand of the $[Ru(tpy)_2]^{2+}$ moiety. [c] In CH_2Cl_2 with a Hg electrode.

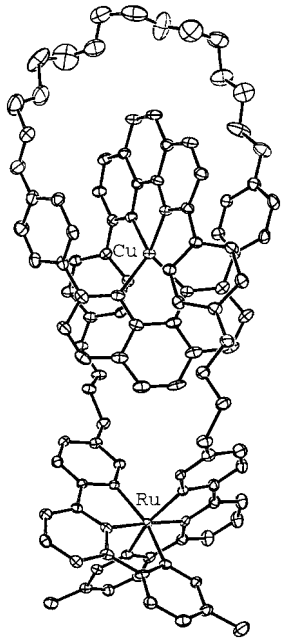

Figure 2. Ortep plot of the cationic part of the **RuCu** compound. Ellipsoids are scaled to enclose 30% of the electronic density. Hydrogen atoms are omitted for clarity.

Adsorption phenomena on the Pt surface may prevent the observation of the electron transfer under such conditions. The use of CH_2Cl_2 as the solvent and a Hg electrode allowed us to detect the irreversible reduction of Ag(I) to Ag(0) (−0.75 V). The value obtained is very similar to the one found for catAg (−0.70 V).[24] **RuZn** exhibits two irreversible waves corresponding to two one-electron redox processes at −0.97 and −1.05 V for the $[Zn(dap)_2]^{2+}$ moiety in accordance with the related catZn.[24] The stabilization of Zn(I) is due to this particular encaged and rigid system since, in the absence of catenand, Zn(II) is directly reduced to Zn(0).

Crystal Structures. The ORTEP drawings for complexes **RuCu** and **RuAg** are depicted in Figures 2 and 3, respectively. The $[Ru(tpy)_2]^{2+}$ fragments show the usual distorted octahedral geometry; the dihedral angles between the tpy ligands are equal to 83.9(1)° and 89.2(1)°. The observed bond distances and angles lie within the range usually shown by this type of complex,[25] which reflects the absence of distortion as compared to similar complexes despite the geometrical restriction imposed by the inclusion of the complex in a macrocycle. This implies that the length of the spacers between the coordinating fragments is enough to allow the existence of a nondistorted interlocked structure. The main differences between both bimetallic complexes are observed in the $[M(dap)_2]^{n+}$ fragment. In both cases

(20) Demas, J. N.; Crosby, G. A. *J. Phys. Chem.* **1971**, *75*, 991.
(21) Nakamaru,K. *Bull. Chem. Soc. Jpn.* **1982**, *55*, 2697.
(22) Flamigni, L. *J. Phys. Chem.* **1992**, *96*, 3331.
(23) Flamigni, L. *J. Phys. Chem.* **1993**, *97*, 9566.
(24) Dietrich-Buchecker, C. O.; Sauvage, J.-P.; Kern, J.-M. *J. Am. Chem. Soc.* **1989**, *111*, 7791.
(25) (a) Beley, M.; Collin, J.-P.; Louis, R.; Metz, B.; Sauvage, J.-P. *J. Am. Chem. Soc.* **1991**, *113*, 8521. (b) Thummel, R. P.; Jahng, Y. *Inorg. Chem.* **1986**, *25*, 2527.

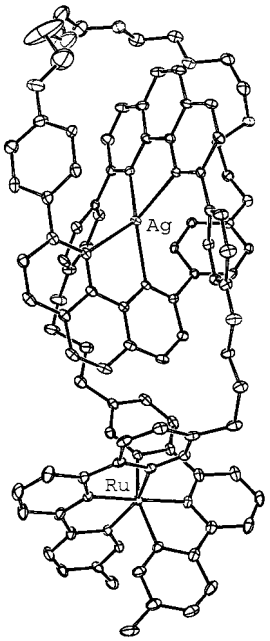

Figure 3. Ortep plot of the cationic part of the **RuAg** compound. Ellipsoids are scaled to enclose 30% of the electronic density. Hydrogen atoms are omitted for clarity.

distorted tetrahedral geometries around the metal centers are observed, but the degree of distortion is different in accord with the different radii of Cu(I) and Ag(I).[26] As a consequence of the bigger size of Ag(I), the angle N−Ag−N for N atoms belonging to the same dap ligand (71.3(3)−73.3(3)°) is smaller than the corresponding bite angle of the Cu complex (81.9(2)°, 82.8(2)°) and the dihedral angles between the mean planes of the dap ligands are, respectively, equal to 62.5(1)° and 85.9-(1)°. This has been observed when the crystal structures of Cu-(I) and Ag(I) complexes of other phenanthroline-type ligands are compared.[27] The Cu−N bond distances (2.029(9)−2.043-(9) Å) are similar to those observed for related complexes,[28] and smaller than the corresponding distances for the Ag(I) derivative (2.316(7)−2.367(7) Å). In both cases, the phenyl ring substituents of the phenanthroline units are oriented facing the other phenanthroline fragments, as was expected according to the high-field chemical shift observed for the aryl hydrogen atoms in the ^{1}H NMR spectra.[14] The metal−metal distances in **RuCu** and **RuAg** are respectively 10.400(1) and 10.177(1) Å and preclude any metal−metal interactions. There are no unusual intermolecular contacts.

Absorption Spectra. The absorption spectra in CH_2Cl_2 solution of **Ru** and **RuCu** are shown in Figure 4. The spectra are characterized in the UV region by the intense ligand-centered (LC) absorption bands of the Ru-based (tpy-type) and cat-based (phen-type) moieties, and in the visible region by the moderately intense Ru → tpy and Cu → phen metal-to-ligand charge-transfer (MLCT) bands.[15,16] In **RuCu** the MLCT absorptions of the [Ru-(tpy)$_2$]$^{2+}$-type and CatCu-type units overlap, but in the 600−700 nm spectral region only the latter moiety absorbs. The spectra of **RuZn** and **RuAg** are very similar to that of **RuCu** in the UV region and to that of **Ru** in the visible region except, in **RuZn**, for the presence of an intense shoulder around 350−400 nm, which is typical of the catZn moiety.[16] In all cases, the spectra of the dinuclear species practically correspond to the sum of the spectra of the model compounds of the two units throughout the UV−vis spectral region.

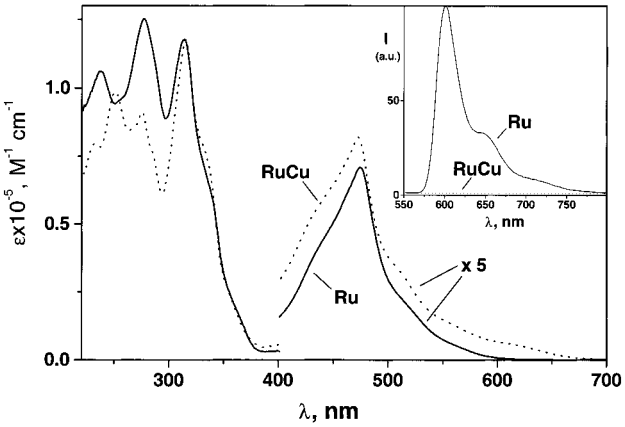

Figure 4. Absorption spectra in CH_2Cl_2 solution at 298 K of compounds **Ru** (solid line) and **RuCu** (dotted line). The inset shows the luminescence spectra of the two compounds in a rigid matrix at 77 K under the same experimental conditions (λ_{exc} = 470 nm). Under appropriate experimental settings, **RuCu** shows weak emission bands centered at 600 and 685 nm (see the text).

Table 3. Luminescence Properties at 298 K[a]

	^{1}LC			^{3}MLCT		
	λ_{max}[b,c] (nm)	τ[d] (ns)	ϕ_{em}[c]	λ_{max}[b] (nm)	τ[d] (ns)	ϕ_{em}[e]
Ru	398	≤0.040[f]	<0.004[g]	615	0.190	∼10^{-5}
cat[h]	400	2.3[i]	0.420			
Ru−Zn	438	≤0.040[f]	<0.001[g]	615	0.130	∼10^{-5}
catZn[h]	463	2.0[j]	0.082			
Ru−Ag				605	0.130	∼10^{-5}
catAg[h]						
Ru−Cu				605	0.110	∼10^{-5}
				750	97[k]	7 × 10^{-4} [l,m]
catCu[h]				730	125	9 × 10^{-4}

[a] Air-equilibrated CH_2Cl_2 solutions, unless otherwise noted. ^{1}LC and ^{3}MLCT are the lowest spin-allowed ligand-centered and the lowest spin-forbidden metal-to-ligand charge-transfer excited states, respectively. [b] From luminescence spectra corrected for photomultiplier response. [c] λ_{exc} = 330 nm. [d] Lifetimes longer than 2.0 ns were measured with the single-photon-counting equipment (λ_{exc} = 337 nm); lifetimes shorter than 2.0 ns were measured with the streak camera (λ_{exc} = 355 and 532 nm for the ^{1}LC and ^{3}MLCT excited states, respectively). [e] λ_{exc} = 470 nm, unless otherwise noted. [f] In butyronitrile. CH_2Cl_2 solutions undergo photodegradation under UV laser irradiation. [g] Partly due to some impurities; see the text. [h] From ref 16. [i] 3.2 ns in BuCN. [j] 3.0 ns in BuCN. [k] 120 ns in oxygen-free solution. [l] 8 × 10^{-4} in oxygen-free solution. [m] Excitation wavelength 440 nm, taking into account only the photons absorbed by the Cu(I)-complexed moiety.

Luminescence Properties. The model compounds exhibit a rich luminescence behavior. In particular cat, catAg, and catZn show[16] ligand-centered fluorescence and/or phosphorescence (^{1}LC, ^{3}LC), whereas for catCu a metal-to-ligand charge-transfer band (^{3}MLCT) is observed.[16] [Ru(tpy)$_2$]$^{2+}$-type compounds display[11,15] a typical ^{3}MLCT emission band, very weak at room temperature and much stronger in a rigid matrix (see Tables 3 and 4). These emission properties of the model compounds can be exploited to determine whether photoinduced intercomponent processes take place in the supramolecular species.

All the investigated compounds exhibit luminescence both in CH_2Cl_2 solution at 298 K and in a CH_2Cl_2 rigid matrix at 77

(26) Ionic radii in tetrahedral complexes: Cu(I), 0.74 Å; Ag(I), 1.14 Å. Shannon, R. D. *Acta Crystallogr.* **1976**, *A32*, 751.

(27) (a) Titze, C.; Kaim, W.; Zalis, S. *Inorg. Chem.* **1997**, *36*, 2505. (b) Titze, C.; Kaim, W. *Z. Naturforsch.* **1996**, *51b*, 981.

(28) (a) Miller, M. T.; Gantzel, P. K.; Karpishin, T. B. *Angew. Chem., Int. Ed. Engl.* **1998**, *37*, 1556. (b) Miller, M. T.; Gantzel, P. K.; Karpishin, T. B. *Angew. Chem., Int. Ed. Engl.* **1998**, *37*, 2285. (c) Cesario, M.; Dietrich-Buchecker, C. O.; Guilhem, J.; Pascard, C.; Sauvage, J.-P. *J. Chem. Soc., Chem. Commun.* **1985**, 244. (d) Dietrich-Buchecker, C. O.; Guilhem, J.; Khemiss, A. K.; Kintzinger, J.-P.; Pascard, C.; Sauvage, J.-P. *Angew. Chem., Int. Ed. Engl.* **1987**, *26*, 661.

Table 4. Luminescence Properties at 77 K[a]

	^{1}LC		^{3}LC		^{3}MLCT	
	λ_{max} (nm)	τ (ns)	λ_{max} (nm)	τ (s)	λ_{max} (nm)	τ (s)
Ru	395[b,c]	0.080[b,d]			602[f]	9.0[g]
cat[e]	382	2.2	524	0.79		
Ru−Zn	418[b,c]	0.100[b,d]			600[f]	8.9[g]
catZn[e]	433	1.0	495	0.78		
Ru−Ag					602[f]	9.2[g]
catAg[e]			498	0.012		
Ru−Cu					600[b,f,h]	0.003[b,i]
					685[b,j]	1.1[b,g]
catCu[e]					685	1.1

[a] CH_2Cl_2 rigid matrix, unless otherwise noted. ^{1}LC and ^{3}LC are the lowest spin-allowed and the lowest spin-forbidden ligand-centered excited states, respectively; ^{3}MLCT is the lowest spin-forbidden metal-to-ligand charge-transfer excited state. [b] Butyronitrile glassy matrix. CH_2Cl_2 solutions undergo photodegradation under UV laser irradiation; see also Table 1. [c] The strongly quenched band could be observed only in the streak image, where the signal-to-noise ratio is much better than in the luminescence steady-state spectrum; $\lambda_{exc} = 355$ nm. [d] $\lambda_{exc} = 355$ nm. [e] From ref 16. [f] $\lambda_{exc} = 470$ nm. [g] $\lambda_{exc} = 337$ nm, single-photon-counting equipment. [h] Very weak signal; see the text. [i] $\lambda_{exc} = 532$ nm. [j] This spectral feature could be observed only in the streak image; for more details see the text.

K. The results obtained are gathered in Tables 3 and 4, along with those of the model compounds. The emission spectra of **Ru** and **RuCu** at 77 K under the same experimental conditions are shown in the inset of Figure 4.

In CH_2Cl_2 solution at 298 K, **Ru** exhibits two very weak emission bands with $\lambda_{max} = 398$ and 615 nm (Table 3), as expected from the luminescence properties of its cat and $[Ru(tpy)_2]^{2+}$ moieties (Figure 1). It should be noted, however, that the cat-type emission is more than 100 times weaker than in the cat model compound. This shows that the lowest singlet excited state of the dianisylphenanthroline (dap) fluorescent units of the cat moiety is strongly quenched by the appended $[Ru(tpy)_2]^{2+}$-type unit. Picosecond luminescence lifetime measurements performed in butyronitrile ($\lambda_{exc} = 355$ nm) show that the residual 400 nm emission is composed by a truly quenched cat-type fluorescence (lifetime shorter than 40 ps) and an unquenched fluorescence signal displaying a lifetime of a few nanoseconds. The presence of less than 1% uncomplexed dap ligands can account for the latter signal. The very weak and short-lived emission with $\lambda_{max} = 615$ nm, characteristic of the $[Ru(tpy)_2]^{2+}$-type compounds,[15] is apparently unaffected by the appended cat moiety, regardless of the excitation wavelength. In a rigid matrix at 77 K (Table 4), the cat-type fluorescence is again strongly quenched, whereas the cat-type phosphorescence, which is very long-lived in the cat model compound (0.79 s), does not appear at all. Upon excitation in the UV or in the visible region, a strong and long-lived emission with $\lambda_{max} = 602$ nm is observed, assigned to the MLCT band of the unperturbed $[Ru(tpy)_2]^{2+}$ moiety. The 77 K excitation spectrum of **Ru**, taken in a transparent glass (CH_2Cl_2/MeOH, 1:1) throughout the UV spectral region ($\lambda_{em} = 602$ nm), matches the corresponding absorption spectrum. The luminescence properties of **RuZn** parallel those of **Ru** (Tables 3 and 4), since the spectroscopic and excited-state properties of catZn are very similar to those of cat.[16]

In the case of **RuAg**, no LC fluorescence can be observed, as happens for the catAg model compound. The lack of ligand-centered fluorescence in catAg was assigned to a very fast intersystem crossing (favored by the presence of the heavy Ag^+ ion), which leads to a relatively long-lived ^{3}LC level ($\tau = 170$ μs at 298 K, measured by transient absorption spectroscopy;[29] $\tau = 12$ ms at 77 K, measured by phosphorescence decay).[16] In

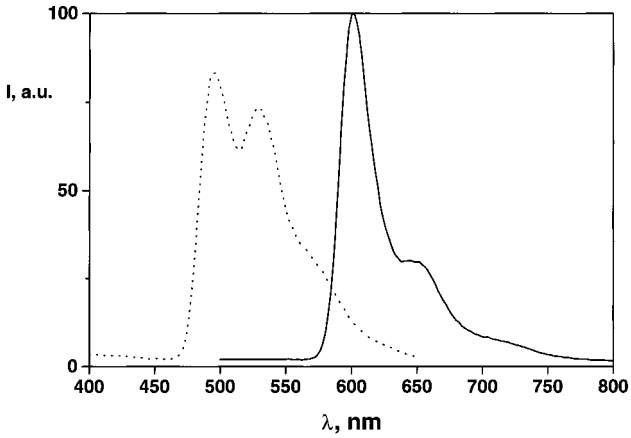

Figure 5. Emission spectra in a CH_2Cl_2 rigid matrix at 77 K of **RuAg** (solid line) and of its model compound catAg (dotted line), under the same experimental conditions. $\lambda_{exc} = 330$ nm.

RuAg, however, we found no trace of a long-lived ^{3}LC level at both 298 and 77 K (Figure 5). In other words in **RuAg**, the catAg moiety is spectroscopically silent, whereas the very weak (at 298 K) and very strong (at 77 K) emissions of the $[Ru(tpy)_2]^{2+}$-type moiety are observed regardless of the excitation wavelength. The excitation spectra of **Ru**, **RuZn**, and **RuAg** taken in a transparent glass (CH_2Cl_2/MeOH, 1:1; $\lambda_{em} = 602$ nm) match the absorption spectra throughout the UV region.

In the case of **RuCu**, it must be recalled that no LC fluorescence and phosphorescence were expected from the catCu moiety, since, as first pointed out by McMillin et al.,[30] the Cu(I)−diimine complexes possess low-energy MLCT excited states. The two lowest ones (^{1}MLCT and ^{3}MLCT) are separated by $\sim$1500 cm^{-1}, and give rise to a broad luminescence band above 700 nm at room temperature. At 298 K **RuCu** shows a broad band with $\lambda_{max} = 750$ nm and $\tau = 120$ ns, similar to that of the catCu model compound;[16] interestingly, the weak $[Ru(tpy)_2]^{2+}$-based emission is not quenched in this case, although its lifetime could not be evaluated with the streak camera device, because it is partially masked by the tail of the MLCT emission of the Cu(I)-complexed moiety. At 77 K, the ^{3}MLCT emission of the $[Ru(tpy)_2]^{2+}$ fragment is dramatically quenched: its lifetime, typically around 9 μs, is lowered to 3 ns (Table 4). Under the same experimental conditions the ^{3}MLCT emission of the catCu moiety is present ($\lambda_{max} = 685$ nm and $\tau = 1.1$ μs),[16] as in the catCu model compound. It is interesting to note that such a spectral feature can be observed only on the streak image, but not in the emission spectrum. The reasons for such a behavior are likely as follows: (a) The 77 K luminescence bands of the $[Cu(phen)_2]^+$-type complexes are extremely weak, even weaker than at room temperature.[31] In the present case the band is weaker than the quenched $[Ru(tpy)_2]^{2+}$-type band. (b) The photomultiplier tube of the spectrofluorimeter (either the R-928 or the R-3896; see the Experimental Section) has a much lower sensitivity around 700 nm than around 600 nm, while the streak camera apparatus has a rather flat response in this spectral range. (c) Long-living unquenched impurities of

(29) Armaroli, N.; Rodgers, M. A. J.; Ceroni, P.; Balzani, V.; Dietrich-Buchecker, C. O.; Kern, J.-M.; Bailal, A.; Sauvage, J.-P. *Chem. Phys. Lett.* **1995**, *241*, 555.

(30) (a) Buckner, M. T.; McMillin, D. R. *J. Chem. Soc., Chem. Commun.* **1978**, 759. (b) Everly, R. M.; McMillin, D. R. *J. Phys. Chem* **1991**, *95*, 9071. (c) Egglestone, M. K.; McMillin, D. R.; Koenig, K. S.; Pallenberg, A. J. *Inorg. Chem.* **1997**, *36*, 172.

(31) Kirchhoff, J. R.; Gamache, R. R., Jr.; Blaskie, M. W.; Del Paggio, A. A.; Lengel, R. K.; McMillin, D. R. *Inorg. Chem.* **1983**, *22*, 2380.

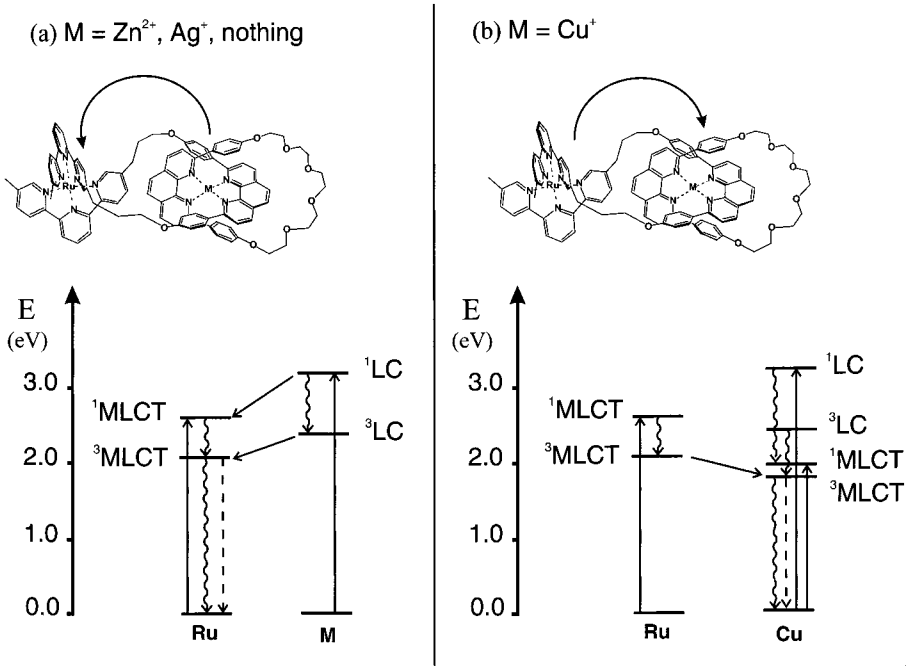

Figure 6. Schematic representation in terms of energy level diagrams of (a) the quenching of ^{1}LC (fluorescent) and ^{3}LC (phosphorescent) excited states of the cat and catM moieties by the $[Ru(tpy)_2]^{2+}$ unit in **Ru**, **RuZn**, and **RuAg** and (b) the quenching of the luminescent ^{3}MLCT excited state of the $[Ru(tpy)_2]^{2+}$ moiety by the catCu moiety in **RuCu**. As one can see the direction of the quenching can be reversed by changing the catenate metal ion. The energy position of each level has been obtained from the maximum of the corresponding emission band at 77 K.

Ru in **RuCu** (<1%), which are evidenced on the streak image, give a strong contribution in the steady-state emission spectrum, but a negligible one in the time-resolved experiment, which explores a time window of only 1.6 ns. These drawbacks prevented the recording of an excitation spectrum of **RuCu** a 77 K.

Photoinduced Intercomponent Energy- and Electron-Transfer Processes. As discussed above, the **Ru**, **RuCu**, **RuZn**, and **RuAg** compounds can be considered to be made of two distinct chromophoric and electroactive units: a $[Ru(tpy)_2]^{2+}$-type complex and a catenand or catenate moiety (Figure 1). Since reliable model compounds of the component units are available, it is possible to highlight the properties resulting from supramolecular (intercomponent) interactions, as previously done for some [3]-catenates and knots.[32−35]

The absorption spectra and the redox properties of the **Ru**, **RuCu**, **RuZn**, and **RuAg** compounds are roughly those expected for the separated components, showing that intercomponent interactions are weak. This result is consistent with the fact that the two moieties are linked by aliphatic chains. It is well-known, however, that even electronic interactions on the order of a few cm^{-1} are sufficient to cause fast intercomponent electron-transfer and exchange energy-transfer processes when the other rate-determining parameters (driving force, $\Delta G°$, and nuclear barrier, λ) have favorable values.[36]

As we have seen above, fast excited-state quenching processes take place in **Ru**, **RuZn**, and **RuAg** upon excitation on the catM moiety; on the contrary, quenching phenomena are observed for the Ru-type fragment in **RuCu**. The rate constant of the quenching process can be calculated from eq 1, where τ and $\tau°$

$$k_q = 1/\tau - 1/\tau° \quad (1)$$

are the excited-state lifetimes of the luminescent moiety in the supramolecular species and in the isolated model compound, respectively. The energy level diagrams needed to discuss the occurrence of energy-transfer processes are shown in Figure 6.[37] As far as electron-transfer processes are concerned, the free energy change involved at 298 K can be estimated from the redox potentials (Table 2) and the excited-state energies of the involved units.[38] In a rigid matrix, the free energy change for the electron-transfer processes are usually much less favorable than in fluid solution, due to the lack of solvent repolarization energy.[39]

For **Ru** and **RuZn**, at 298 K, the ^{1}LC fluorescence of the cat and catZn moieties is strongly quenched by the $[Ru(tpy)_2]^{2+}$-

(32) Armaroli, N.; Balzani, V.; Barigelletti, F.; De Cola, L.; Sauvage J.-P.; C. Hemmert *J. Am. Chem. Soc.* **1991**, *113*, 4033.

(33) Armaroli, N.; Balzani, V.; Barigelletti, F.; De Cola, L.; L. Flamigni; Sauvage J.-P.; Hemmert, C. *J. Am. Chem. Soc.* **1994**, *116*, 5211.

(34) Armaroli, N.; Balzani, V.; De Cola, L.; Hemmert, C.; Sauvage J.-P. *New J. Chem.* **1994**, *18*, 775.

(35) Dietrich-Buchecker, C. O.; Sauvage, J.-P.; Armaroli, N.; Ceroni, P.; Balzani, V. *Angew. Chem., Int. Ed. Engl.* **1996**, *35*, 1119.

(36) Barbara, F. P.; Meyer T. J.; Ratner, M. A. *J. Phys. Chem.* **1996**, *100*, 13148.

(37) The energy values indicated in Figure 6 are typically estimated from the maxima of the emission band at 77 K. Such values are only indicative for ^{1}LC and ^{3}LC, whose energy content is slightly affected by different complexing ions (Table 4). For the Cu-type moiety ^{3}MLCT has been estimated from the 77 K emission maximum of the reference compound catCu (ref 16), whereas 1500 cm^{-1} has been added to locate ^{1}MLCT (see the text). For the Ru-type moiety ^{1}MLCT and ^{3}MLCT have been determined from the absorption and 77 K emission spectra of **Ru**, respectively.

(38) For a generic excited-state electron-transfer reaction, $A^* + B \rightarrow A^- + B^+$, the thermodinamic driving force can be evaluated from the approximate equation $\Delta G° \cong -\Delta E°° - E(A/A^-) + E(B^+/B)$, where $E(A/A^-)$ and $E(B^+/B)$ are the energies (eV) of the one-electron reduction processes and $\Delta E°°$ is the spectroscopic energy, taken as the energy of the maximum of the emission spectrum at 77 K. If we indicate, for our compounds, the single moieties with just their complexing ion (using cat for the uncomplexed moiety of **Ru**), we have $\Delta E_{cat}°° = 3.10$ eV, $\Delta E_{Zn}°° = 2.86$ eV, $\Delta E_{Ag}°° = 2.49$ eV, $\Delta E_{Ru}°° = 2.07$ eV, and $\Delta E_{Cu}°° = 1.77$ eV. If we put into the above equation the proper electrochemical potentials (see Table 2), the only thermodynamically allowed photoinduced electron-transfer processes are the following: Ru^+-Cu^{2+} (excitation on the Ru moiety, $\Delta G° = -0.17$ eV); $Ru^{3+}-Zn^+$ (excitation on the Zn moiety, $\Delta G° = -0.62$ eV); $Ru^{3+}-Ag^0$ (excitation on the Ag moiety, $\Delta G° = -0.77$ eV; excitation on the Ru moiety, $\Delta G° = -0.35$ eV).

(39) Chen P.; Meyer T. J. *Inorg. Chem.* **1996**, *35*, 5520.

based moiety (Table 3). From eq 1, the quenching rate constants are $>5 \times 10^{10}$ s^{-1}. In the case of **Ru**, both the oxidative and reductive electron-transfer processes betwen the ^{1}LC excited state of the cat moiety and the ground-state Ru(II) complex are endoergonic, and therefore they cannot account for such fast quenching processes. As shown in Figure 6a, energy transfer is energetically allowed for **Ru**, and it can account for the observed quenching process. In view of the relatively intense absorption of the acceptor in the spectral region of the donor emission, fast energy transfer could also occur by a Coulombic mechanism.[40] Unfortunately, the emission of the $[Ru(tpy)_2]^{2+}$ acceptor is too weak to have direct proof of the occurrence of energy transfer from the excitation spectrum. In the case of **RuZn**, oxidative electron-transfer quenching of the Ru(II) center is thermodynamically allowed, but only upon excitation of the catZn moiety;[38] this could perhaps contribute to the quenching process of ^{1}LC at 298 K. At 77 K, for both **Ru** and **RuZn**, complete quenching of the ^{1}LC and ^{3}LC levels of the cat and catZn moieties is observed, and it can be accounted for by an energy transfer to the MLCT levels of the $[Ru(tpy)_2]^{2+}$ moiety (Figure 6a), which turns out to be sensitized in the excitation spectra. In the case of the ^{3}LC phosphorescent level, the energy-transfer quenching mechanism is most likely of the exchange type.[40b]

For **RuAg**, at 298 K oxidative electron-transfer quenching of the Ru(II) center is thermodynamically allowed regardless of the excited component[38] so that a contribution of such a mechanism to the observed complete fluorescence quenching of the catAg unit cannot be ruled out. In a rigid matrix at 77 K, the lack of fluorescence can be due either to a complete quenching via energy transfer or to a fast intersystem crossing, as happens for the catAg model compound. Since sensitization of the ^{3}MLCT Ru(II)-based emission is observed, in the second case the lack of phosphorescence can again be accounted for by an exchange energy transfer to the ^{3}MLCT level of the $[Ru(tpy)_2]^{2+}$ moiety (Figure 6a).

In the case of **RuCu**, the picture is different because the lowest excited state is no longer the ^{3}MLCT level of the $[Ru(tpy)_2]^{2+}$ moiety, but the ^{3}MLCT level of the catCu one (Figure 6b). A key result to understand what happens in this compound is that obtained upon excitation of the ^{1}MLCT level of the $[Ru(tpy)_2]^{2+}$ moiety. At 298 K this excited state is very short-lived ($1/\tau^\circ =$ ca. 1×10^{10} s^{-1}), so that quenching processes can hardly compete; accordingly, the excitation spectrum of **RuCu**, read at 720 nm, does not receive any appreciable contribution from the $[Ru(tpy)_2]^{2+}$-based absorption bands in the visible spectral region. On the contrary, at 77 K, the $[Ru(tpy)_2]^{2+}$-based emission is dramatically quenched, with a rate constant of 3×10^8 s^{-1}; unfortunately the excitation spectrum read on the Cu(I)-based emission could not be recorded, for the reasons previously outlined. Nevertheless, the observed quenching can be assigned to an energy-transfer mechanism. In fact, at 298 K, the electron transfer (corresponding to the reduction and oxidation of the Ru(II) and of the Cu(I) metal center, respectively) is exergonic, only by 0.17 eV,[38] a value most likely not sufficent to allow electron transfer also in a 77 K rigid matrix, where the effective solvent dielectric constant decreases dramatically because the solvent dipoles cannot reorient to stabilize the newly formed ions.[39]

Energy Transfer to Dioxygen. In fluid solution at room temperature the luminescent ^{3}MLCT excited state of the Cu(I)−bisphenanthroline-type complexes is quenched by dioxygen.[33] The quenching constant $k_q[O_2]$ of **RuCu** (2.1×10^6 s^{-1}) is quite similar to that of catCu (2.4×10^6 s^{-1})[33] in CH_2Cl_2 solution. This is an expected result, as the two compounds bear the same chelating ligand (2,9-*p*-dianisyl-1,10-phenanthroline) on the Cu(I) ion,[41] whereas differences in the oxygen quenching constants are only observed upon strong changes of the steric hindrance and electronic properties of the phenanthroline substituents.[33] We have also found that, in **RuCu**, the quenching process is accompanied by the sensitization of the $^1\Delta(O_2)$ emission at 1269 nm, with a relative quantum yield of singlet oxygen generation comparable to that of catCu. This is likely to reflect a similar energy-transfer quenching mechanism in the two cases, although a second deactivation pathway, i.e., eletron transfer, cannot be ruled out as already discussed.[33]

Conclusions

A new family of four [2]-catenates have been prepared and characterized. They consist of two interconnected moieties, an octahedral ($[Ru(tpy)_2]^{2+}$-type) and a tetrahedral ($[M(phen)_2]^{n+}$-type) species. In the latter M can be Cu^+, Zn^{2+}, or Ag^+, but such a moiety can also be metal free. The electrochemical, X-ray, and UV−vis properties show that the two units do not interact appreciably. However, photoinduced excited-state intercomponent interactions cause energy- and/or electron-transfer processes. The direction of such transfer processes can be reversed upon a suitable choice of the metal ion complexing the $[M(phen)_2]^{n+}$-type coordination center. When $M^{n+} = Zn^{2+}$, Ag^+, or nothing, the excited states of the tetrahedral moiety can be quenched by energy- and/or electron-transfer processes to the octahedral one, at both 298 and 77 K; when $M^{n+} = Cu^+$, energy transfer is observed in the opposite direction at 77 K. The nature of the lowest excited states can be LC or MLCT (singlets or triplets) (Figure 6), and the energy can be varied in the range 3.1−1.6 eV (400−750 nm). These results show that the $[M(phen)_2]^{n+}$ unit can be a valuable building block for constructing supramolecular architectures offering a high degree of control over energy- and electron-transfer pathways. We believe that such potentiality has not yet been fully exploited. Finally it must be pointed out that reversible protonation of the free bisphenathroline unit can also be performed, thus introducing a further opportunity to tune excited-state energy.[16,34,42,43] Studies along those directions are underway in our laboratories.

Acknowledgment. This work was supported by CNR (Italy), MURST (Italy), the University of Bologna (Funds for Selected Research Topics), CNRS (France), and EU (TMR Grant FMRX-CT-96-0031). D.J.C. and P.G. thank the Ministerio de Educación y Ciencia (Spain) and the European Union for their financial support. We thank M. Minghetti and L. Ventura for technical assistance.

Supporting Information Available: Tables S1−S12, listing full crystallographic data, atomic coordinates, equivalent isotropic thermal and anisotropic temperature parameters, and bond distances and angles for **RuCu** and **RuAg** and Ortep plots of the cationic parts of **RuCu** and **RuAg** (PDF). An X-ray crystallographic file, in CIF format, is available through the Internet only. This material is available free of charge via the Internet at http://pubs.acs.org.

JA990036V

(40) (a) Förster, Th. *Discuss. Faraday Soc.* **1959**, *27*, 7. (b) Turro, N. J. *Modern Molecular Photochemistry*; Benjamin: Menlo Park, CA, 1978.

(41) Dietrich-Buchecker, C. O.; Nierengarten, J.-F.; Sauvage, J.-P.; Armaroli, N.; Balzani, V.; De Cola, L. *J. Am. Chem. Soc.* **1993**, *115*, 11237.

(42) Armaroli, N.; De Cola, L.; Balzani, V.; Sauvage, J.-P.; Dietrich-Buchecker, C. O.; Kern, J.-M. *J. Chem. Soc., Faraday Trans.* **1992**, *88*, 553.

(43) Dietrich-Buchecker, C. O.; Sauvage, J.-P.; Armaroli, N.; Ceroni, P.; Balzani, V.; Kern, J.-M. *New J. Chem.* **1996**, *20*, 801.